Electronic supplementary information for

Characterization of visible-light photo-Fenton reaction using Fe-doped ZnS (Fe$_x$-ZnS) mesoporous microspheres

Qiao Wang[a], Peng Xu[a], Guangshan Zhang[a],*, Wen Zhang[b], Limin Hu[a], Peng Wang[a],*

[a]*State Key Laboratory of Urban Water Resource and Environment, School of Environment, Harbin Institute of Technology, Harbin 150090, China*

[b]*John A. Reif, Jr. Department of Civil & Environmental Engineering, New Jersey Institute of Technology, Newark, NJ 07102, USA*

*Corresponding authors. Address: School of Environment, Harbin Institute of Technology, No. 73 Huanghe Road, Nangang District, Harbin 150090, China.

E-mails: gszhanghit@gmail.com (G. S. Zhang), pwang73@vip.sina.com (P. Wang).

Tel./Fax: +86 451 86283557.

This electronic supplementary information (ESI) contains the following sections:

S1. Schematic diagram of photocatalytic reactor (Fig. S1).

S2. UV-Vis adsorption spectrum and standard curve of PNP (Fig. S2).

S3. Grain size distribution of $Fe_{10\%}$-ZnS photocatalyst (Fig. S3).
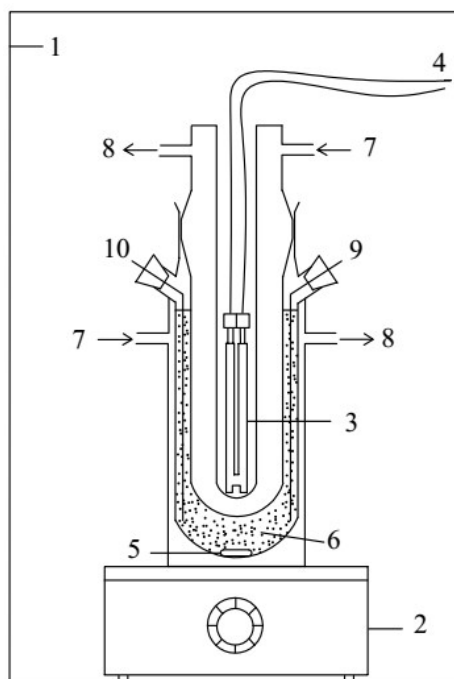
S4. Plots of $(Ahv)^2$ versus hv (Fig. S4).

S5. Degradation efficiencies of RhB in different reaction systems (Fig. S5)

S6. Degradation efficiencies of PNP in homogeneous $Fe^{3+}/H_2O_2/Vis$ system (Fig. S6)
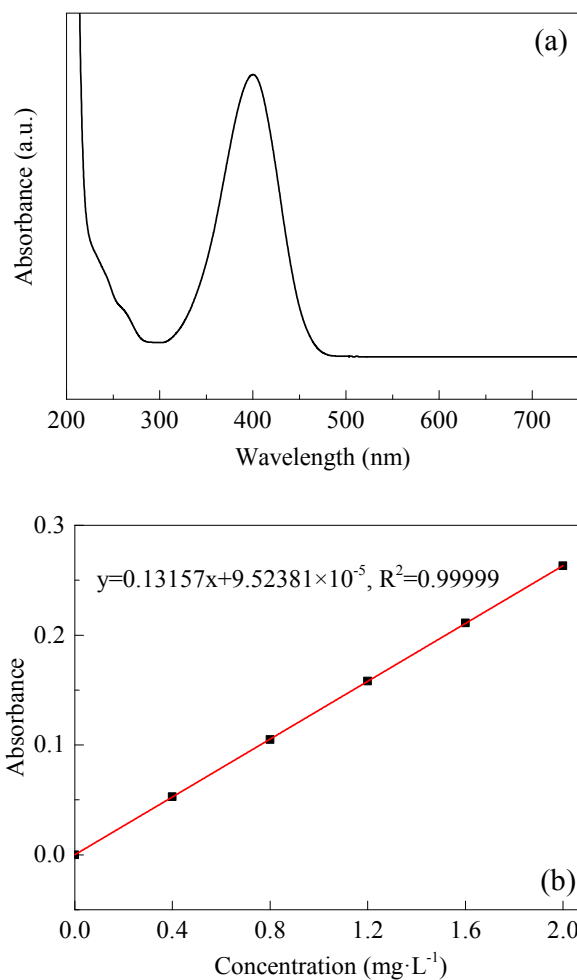
S7. Mass transfer calculations.

S1. Schematic diagram of photocatalytic reactor

**Fig. S1.** Schematic diagram of photocatalytic reactor.

(1. Metal shield; 2. Magnetic stirrer; 3. Light source; 4. Electrical source; 5. Rotor;
6. Solution; 7. Cooling water in; 8. Circulating water out; 9. Gas in; 10. Sampling port.)

## S2. UV-Vis adsorption spectrum and standard curve of PNP

Fig. S2. (a) UV-Vis adsorption spectrum of initial PNP solution at pH>11; (b) Standard curve of PNP, where x is the PNP concentration and y is the corresponding absorbance.

S3. Grain size distribution of Fe$_{10\%}$-ZnS photocatalyst
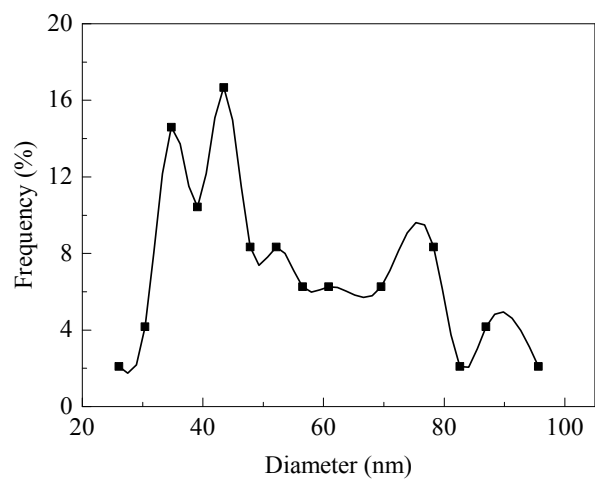
Fig. S3. Grain size distribution of Fe$_{10\%}$-ZnS photocatalyst based on the statistical measurement (more than 40 grains were counted) from the FESEM image.
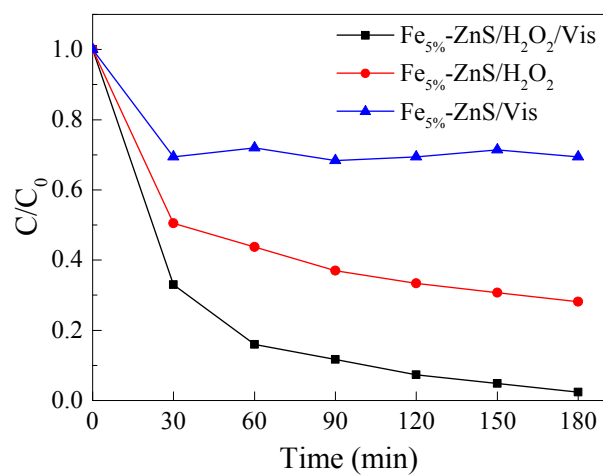
S4. Plots of (A*hv*)² versus *hv*
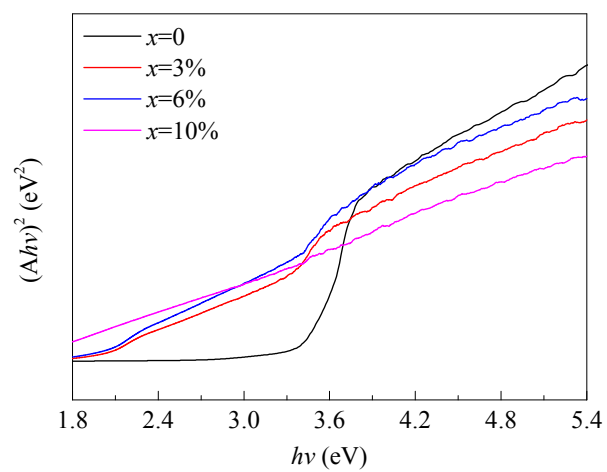
Fig. S4. Plots of (A*hv*)² versus *hv* according to the UV-Vis spectra.

## S5. Degradation efficiencies of RhB in different reaction systems

The photocatalytic activity was also detected through the degradation of rhodamine B

(RhB, a common azo dye and normally adopted to test the performance of photocatalyst).

Fig. S5. Degradation efficiencies of RhB in different reaction systems.

(Under the conditions of an initial RhB concentration of 10 mg·L^{-1}, a catalyst dosage of 0.8 g·L^{-1} and a H$_2$O$_2$ concentration of 2 mmol·L^{-1}.)

S6. Degradation efficiency of PNP in homogeneous $Fe^{3+}/H_2O_2/Vis$ system

According to the doping molar ratio of Fe^{3+} (6%) in the Fe_x-ZnS catalyst and the catalyst dosage of 0.8 $g \cdot L^{-1}$, the Fe^{3+} ion concentration in the homogeneous $Fe^{3+}/H_2O_2/Vis$ system was calculated as 0.028 $g \cdot L^{-1}$. The final degradation efficiency of PNP was 68.0% within 180 under visible light irradiation.
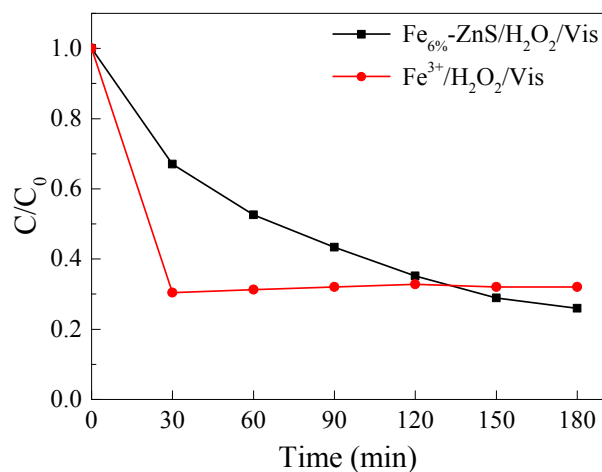
Fig. S6. Comparison of heterogeneous $Fe_{6\%}$-ZnS /H_2O_2/Vis system and homogeneous Fe^{3+}/H_2O_2/Vis system on PNP degradation efficiency.
(Under the conditions of an initial PNP concentration of 10 $mg \cdot L^{-1}$, a Fe^{3+} concentration of 0.028 $g \cdot L^{-1}$ and a H_2O_2 concentration of 2 $mmol \cdot L^{-1}$.)

S7. Mass transfer calculations

S7.1. Aqueous/solid mass transfer limitations

The slip velocity method described previously was used to estimate the minimum expected k_{aq}, because this method calculates the mass transfer rate constant (k_{aq}) for particles traveling at the slip velocity (u_t) relative to the suspending liquid at high stirring rates were used. The particle's slip velocity was calculated by the Stokes Law:

$$u_t = \frac{gd_p^2(\rho_p - \rho)}{18\mu} \tag{S1}$$

where g is the gravity constant (9.8 N·kg^{-1}), d_p and ρ are the diameter (in average) and density (3.9×10^6 kg·m^{-3}) of the catalyst particle, respectively, ρ is the density of water (9.97×10^5 kg·m^{-3}), and μ is the absolute viscosity of water (0.89 g·m^{-1}·s^{-1}). The aqueous/solid mass transfer coefficients were then estimated by:

$$k_{aq} = \frac{D_{mol}}{d_p}Sh = \frac{D_{mol}}{d_p}\left(2 + 0.6Re^{0.5}Sc^{0.33}\right) \tag{S2}$$

where D_{mol} is the molecular diffusion coefficient (cm^2·s^{-1}) of the reacting solute (e.g, PNP), Sh is the Sherwood number, Re is the modified Reynold's number, and Sc is the Schmitt number. The molecular diffusion coefficient for PNP in water were calculated using the method in Hayduk and Laudie:

$$D_{mol} = \frac{13.26 \times 10^{-5}}{\mu^{1.14}(v')^{0.589}} \tag{S3}$$

where   is the molar volume of the reacting solute (cm^3·mol^{-1}), which was calculated by the LeBas method as shown in Table S1.

Table S1. Calculations of molar volumes for PNP using the LeBas Method.

PNP	Atomic volume	Number	Total
Carbon	14.8	6	88.8
Hydrogen	3.7	5	18.5
Nitrogen	17.3	1	17.3
Oxygen	7.4	3	22.2
		=	146.8

Reynolds's number and Schmitt number are calculated by:

$$Re = \frac{d_p u_t}{\nu_{H_2O}} \tag{S4}$$

$$Sc = \frac{\nu_{H_2O}}{D_{mol}} \tag{S5}$$

$$Sh = 2 + 0.6 Re^{0.5} Sc^{0.33} \tag{S6}$$

where ν_{H_2O} is the kinematic viscosity of water (8.93×10^{-7} g·m^{-1}·s^{-1} at 25 °C).

The mass transfer rate constants were then calculated by multiplying the mass transfer coefficients by the geometric surface area of the catalyst per volume of solution. a (m^{-1}) is the geometric surface area of the catalyst per volume of solution:

$$a = \frac{SA_P \times M}{\rho_P \times V_P} \times \frac{1}{V_R} \tag{S7}$$

where SA_p (m^2) is the geometric surface area of one particle, M (g) is the mass of catalyst in the reactor, V_p (m^3) is the geometric volume of one particle, and V_R (0.25 L) is the reactor volume.

Reaction rate constant k_{obs} (s^{-1}) can be calculated in Eq. (S8):

$$k_{obs} = -\frac{Ln\frac{[A]_t}{[A]_0}}{t} \tag{S8}$$

where $[A]_t$ and $[A]_0$ is the concentration of reactant at time t and 0 s, respectively. T (s)

is the reaction time.

S7.2. Intraparticle mass transfer limitations

No resistance to pore diffusion if

$$\frac{k_{obs}L^2}{De} < 1 \qquad (S9)$$

Significant resistance to pore diffusion if

$$\frac{k_{obs}L^2}{De} > 1 \qquad (S10)$$

where L is the characteristic diffusion pathlength for the catalyst and De is the effective diffusivity of the reacting solute.

Eqs. (S9) and (S10) provide a general measure of the characteristic time scale for diffusion relative to the characteristic time scale for reaction. A calculated value significantly less than one indicates that diffusion is fast compared to the observed reaction. L and De were estimated using the following expressions:

$$L = \frac{1}{6}d_p \qquad (S11)$$

$$De = \frac{D_{mol}\theta}{tau} \qquad (S12)$$

The most conservative values from each range were used to maximize the possibility that the criterion in Eqs. (S11)-(S12). The smallest θ (0.2) and largest tau (τ) (10) were chosen in order to obtain the smallest possible De value, and, in turn, the largest possible value for Eqs. (S9)-(S10).